Electronic Supplementary Information (ESI) for

Photoswitchable Alkoxy-Bridged Binuclear Rhenium(I) Complexes – A Potential Probe for Biomolecules and Optical Cell Imaging

Veerasamy Sathish,[a] Eththilu Babu,[a] Arumugam Ramdass,[a] Zong-Zhan Lu,[b] Tzu-Ting Chang,[b] Murugesan Velayudham,[b] Pounraj Thanasekaran,[b] Kuang-Lieh Lu,*[b] Wen-Shan Li,*[b] and Seenivasan Rajagopal*[a]

[a]*Department of Physical Chemistry, School of Chemistry, Madurai Kamaraj University, Madurai, Tamilnadu, India*

[b]*Institute of Chemistry, Academia Sinica, Taipei 115, Taiwan*

Table S1. Crystallographic data of **1**.

	1
empirical formula	$C_{48}H_{44}N_2O_8Re_2$
M_w	1149.27
crystal system	orthorhombic
space group	$P2_12_12_1$
a (Å)	14.0169(3)
b (Å)	16.7072(3)
c (Å)	19.0984(4)
V (Å^3)	4472.52(16)
Z	4
T (K)	296
λ (Å)	0.71073
D_{calc} (g cm^{-3})	1.707
μ (mm^{-1})	5.463
Flack parameter	[0.005(16)]
F_{000}	2240
GOF	1.073
R_1[a] ($I > 2\sigma(I)$)	0.0483
wR_2[b] ($I > 2\sigma(I)$)	0.1223
R_1[a] (all data)	0.0595
wR_2[b] (all data)	0.1154
$\Delta\rho_{max}/\Delta\rho_{min}$ (e Å^{-3})	2.069/-1.351

[a]$R_1 = \sum||F_0| - |F_c||/\sum|F_0|$. [b]$wR_2 = \{\sum[w(F_0^2 - F_c^2)^2]/\sum[w(F_0^2)^2]\}^{1/2}$.

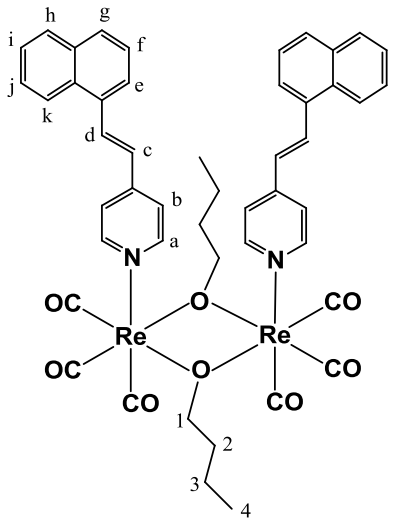

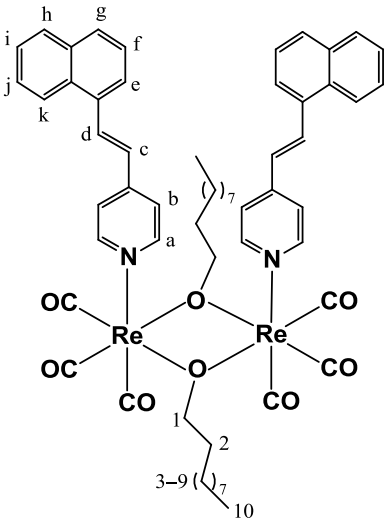

Scheme S1. ^{1}H NMR numbering for complexes **1** and **2**.

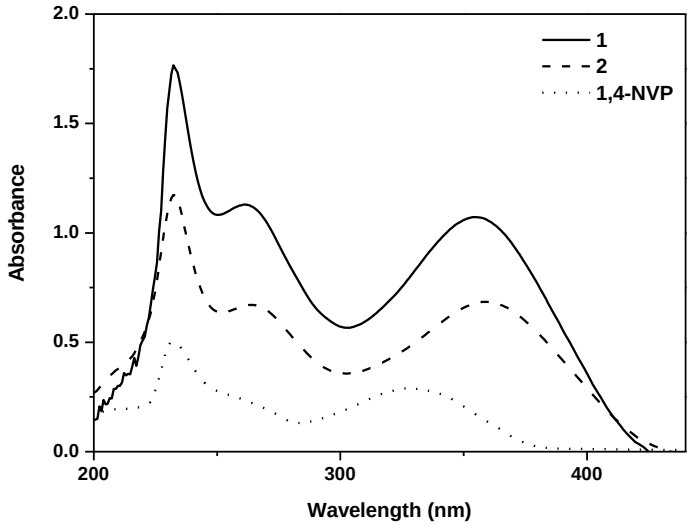

Figure S1. UV–vis spectra of complexes **1** (solid line) and **2** (dash line) and free ligand 1,4-NVP (dot line) in CH_2Cl_2.

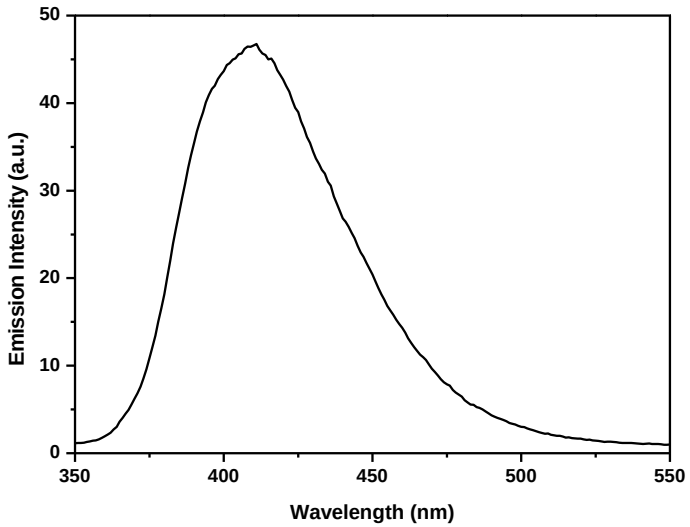

Figure S2. Emission spectrum of 4-(1-naphthylvinyl)pyridine ligand in CH_2Cl_2.

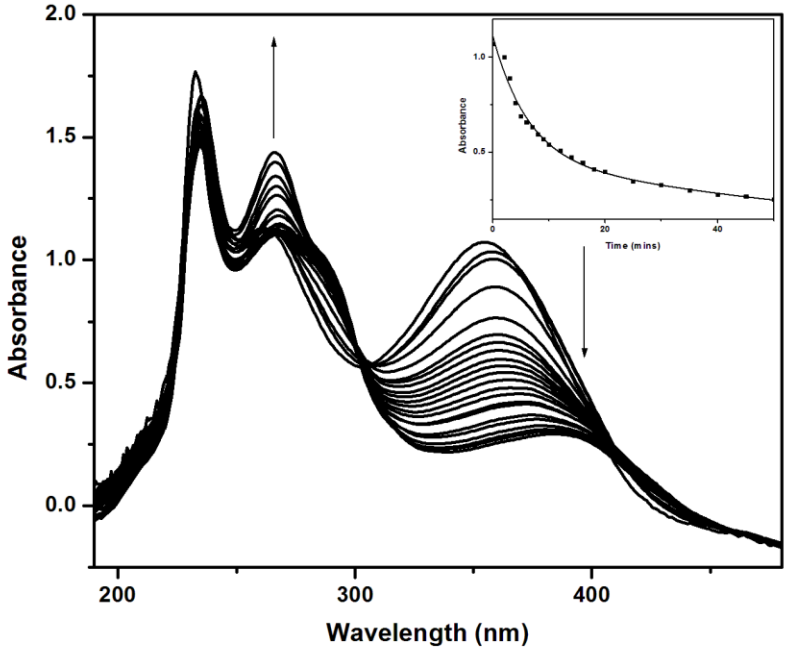

Figure S3. UV–vis spectral changes of complex **1** (3×10^{-5} M) in CH_2Cl_2 upon irradiation at 365 nm.

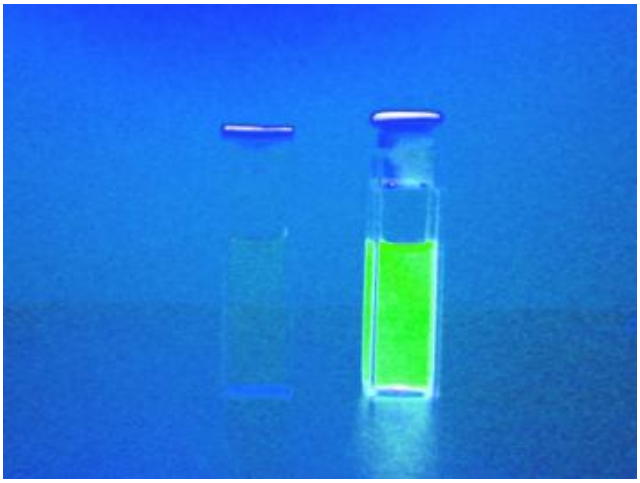

Figure S4. Photograph taken before and after the irradiation of **2** under illumination from a UV lamp at 365 nm in CH_2Cl_2.

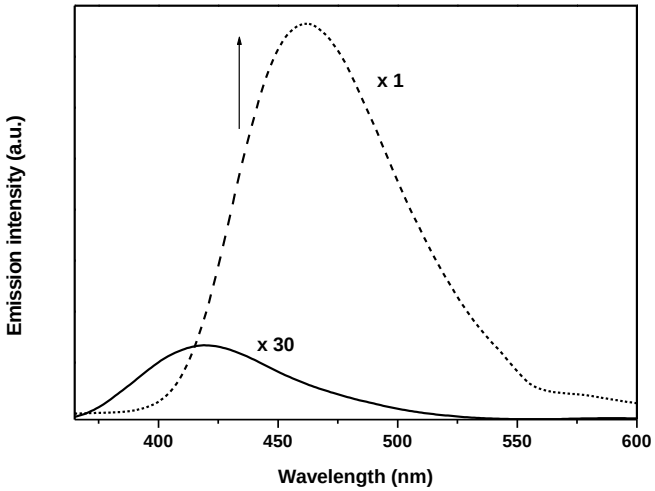

Figure S5. Emission spectra of **2** (3×10^{-5} M) before (——) and after (-----) photolysis in CH_2Cl_2.

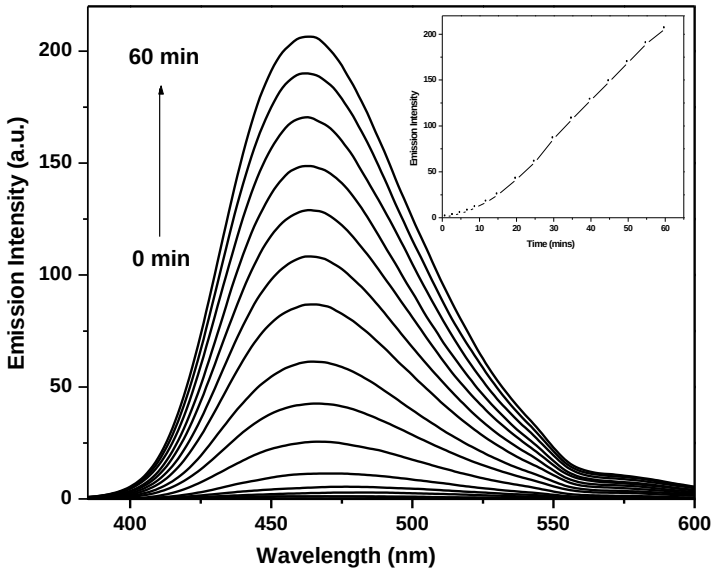

Figure S6. Enhancement in emission intensity upon 365 nm irradiation of complex **1** (3×10^{-5} M) in CH_2Cl_2.

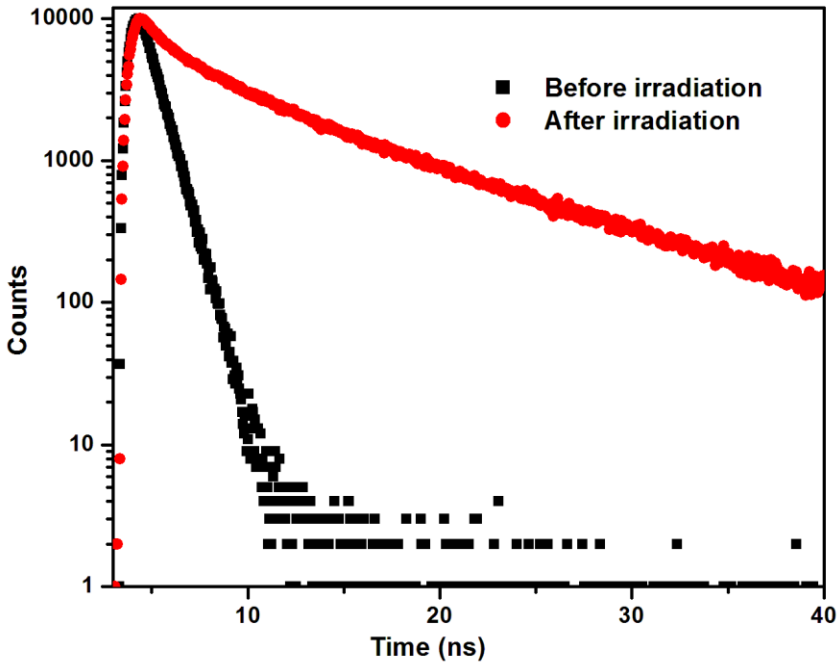

Figure S7. Lifetime decay profiles of **2** in CH_2Cl_2 before (black line) and after (red line) irradiation.

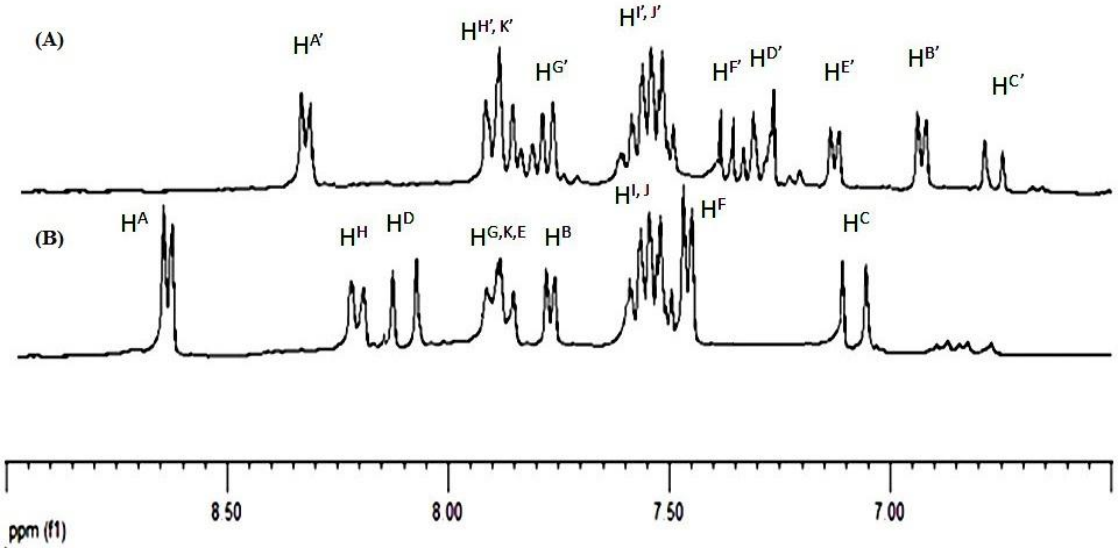

Figure S8. ^1H NMR spectra of complex **2** after (A) and before (B) irradiation at 365 nm in $CDCl_3$.

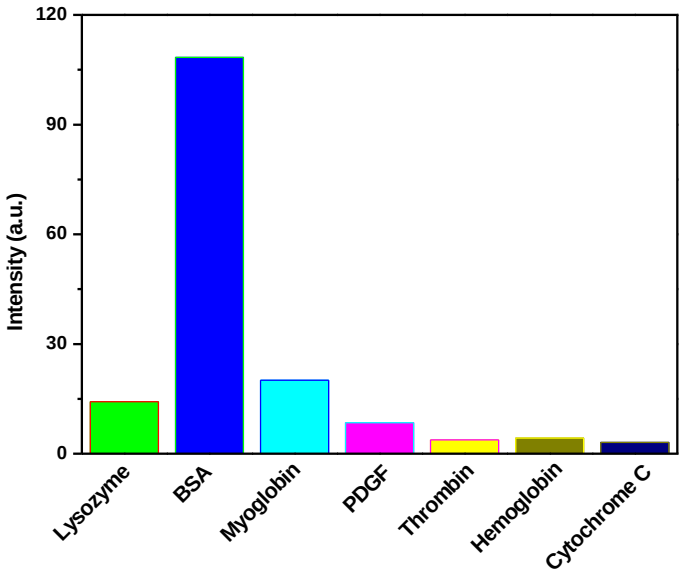

Figure S9. Comparison of the fluorescence intensity of **2** (20 μM) in the presence of various proteins.

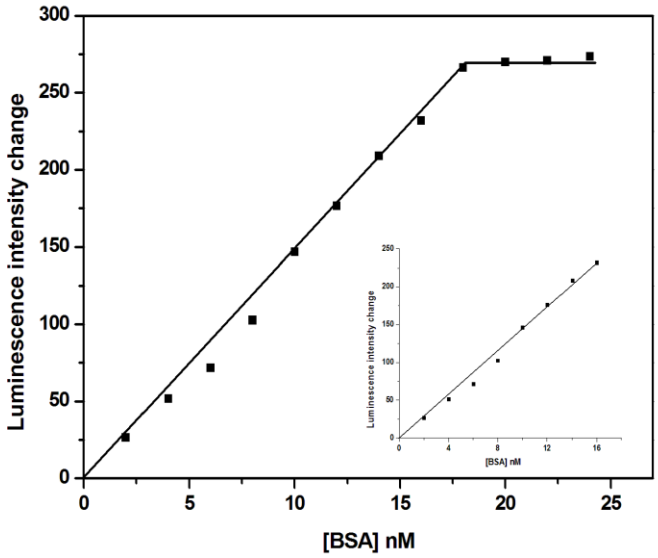

Figure S10. Luminescence intensity change of complex **2** *versus* [BSA] in PBS buffer. The concentration of BSA is 0 –24 × 10^{-9}M. Inset: calibration plot of BSA sensor (R =0.993).

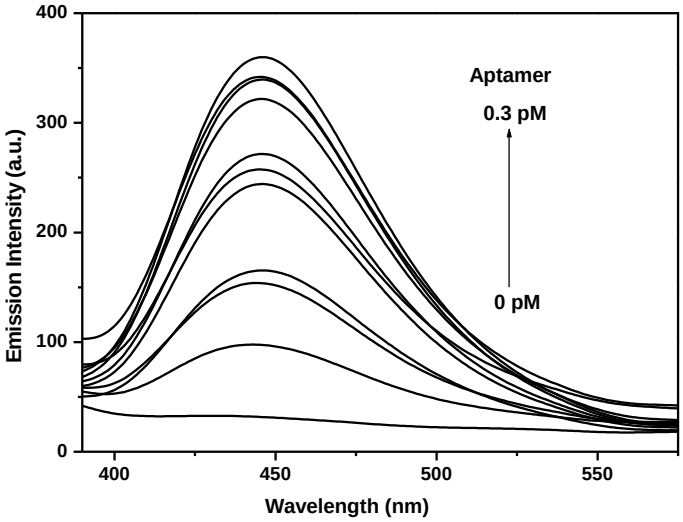

Figure S11. Emission spectral changes of complex **1** (10 μM) with the addition of PDGF aptamer (0 pM to 0.3 pM) in PBS buffer.

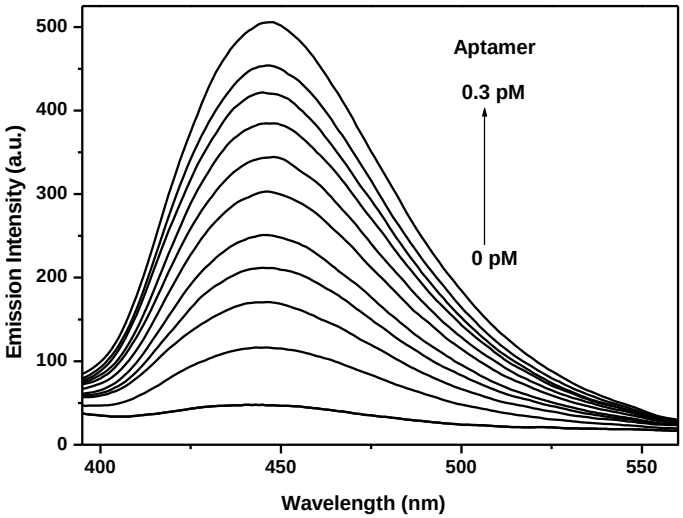

Figure S12. Emission spectral changes of **2** (10 μM) with the addition of PDGF binding aptamer (0 pM to 0.3 pM) in PBS buffer (pH = 7.4).

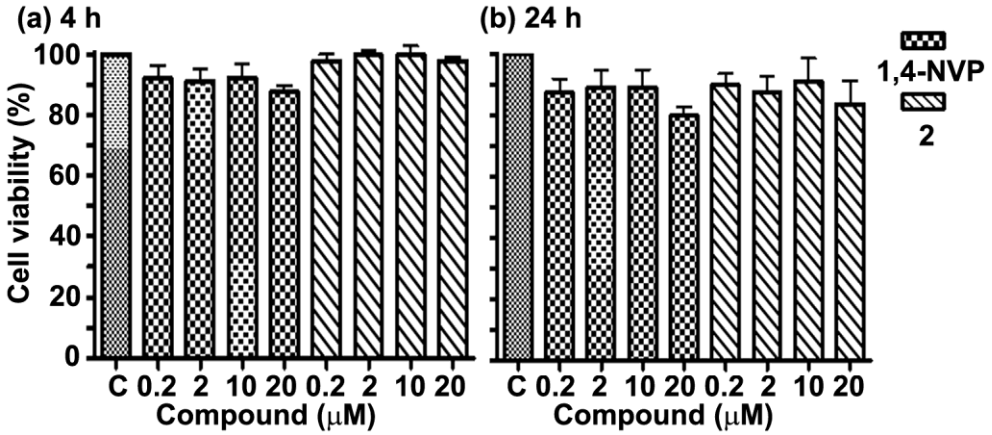

Figure S13. *In vitro* cell viability effects of 1,4-NVP and rhenium(I) complex **2** in inhibiting the growth of breast epithelium cells, M10, at 4 and 24 h..